Bilateral teleoperation: quantifying the requirements for and restrictions of ideal transparency

Bert Willaert, Dominiek Reynaerts, Hendrik Van Brussel and Emmanuel B. Vander Poorten

***Abstract*—The well-known trade-off between transparency and stability challenges the realization of bilateral teleoperation systems. Ideal conditions for the four-channel framework have been presented, but the practical feasibility is hardly quantified. This paper bridges the gap between existing detailed analysis of basic two-channel controllers and the ideal conditions for the four-channel framework.**

Starting from the fundamental stability and transparency limits of the Position-Force controller, two extensions of this controller have been analyzed in detail, using existing metrics for transparency and the absolute stability and bounded environment passivity criterion. This analysis quantitatively describes the effect of hardware properties, modelling errors and low-pass filters and illustrates as such the restrictions on the realization of ideal transparency. The experimental results presented in this paper, demonstrate the restricted stiffness transparency of the Position-Force controller, as well as how the extensions provide close to perfect stiffness transparency.

***Index Terms*—Bilateral Teleoperation, Passivity, Transparency**

I. Introduction

A bilateral teleoperation system allows a human operator to manipulate a (remote) environment through a master and slave robotic device, while also feeling the environment. This feeling can make teleoperation more intuitive, faster and more precise. However, the user's desire to feel directly connected to the environment is typically opposed to the need for stable interactions under all operating conditions. This well-known trade-off between transparency and stability challenges the realization of bilateral teleoperation systems.

The ideal bilateral teleoperation system acts as a massless, infinitely stiff connection between the end-effector of the master and the slave [1]. This system would provide perfect transparency, i.e. a one-to-one mapping between the environment impedance and the impedance felt by the human operator, while being also two-port passive. This implies that the interaction with all possible passive environments and operators is guaranteed stable. However, as stated in literature and as will be illustrated throughout this paper, realizing this ideal bilateral teleoperation system is practically impossible independent of the control architecture.

In the beginning of the nineties, Lawrence in [2] and Yokokohji and Yoshikawa in [3] presented a manner to generalize different control architectures. In [4], Hashtrudi-Zaad and Salcudean extended Lawrence's four-channel framework with a local force-feedback loop for both the master and the slave (C_5 and C_6). This extended four-channel framework became the basis for numerous research efforts. The transparency properties of this four-channel framework have been discussed thoroughly in [4]–[6] and also the stability properties received quite some attention. The detailed stability analyses in [2], [7]–[11] are, however, restricted to two-channel controllers, while the analyses of more complex controllers in [3], [8], [12] are limited to numerical examples and lack the description of (analytic) tuning or hardware design guidelines.

In order to obtain the aforementioned ideal teleoperation system, the following conditions have been derived for the parameters of the four-channel framework [2], [3], [7]:

$$\begin{cases} C_1 = & Z_s + C_s & C_2 = 1 + C_6 \\ C_3 = & 1 + C_5 & C_4 = -(Z_m + C_m) \end{cases} \quad (1)$$

The physical interpretation of these *ideal* conditions is the following: the first and fourth condition ensure that the master and slave dynamics are cancelled out using inverse dynamics. The second and third condition ensure that the net effect of F_h and F_e is the same for both the master and the slave. These ideal conditions require an exact knowledge of the master and slave dynamics as well as an exact measurement of acceleration and force signals. This already illustrates why realizing the ideal bilateral teleoperation system is practically impossible. In this context, it is also interesting to understand that this ideal teleoperation system is not strictly two-port passive but *lossless*. It is a border case of the set of passive systems. Hence, the smallest error in (i) the estimate for the dynamic models or in (ii) the measurement of acceleration and force, e.g. due to the use of a low-pass filter introducing phase lag, can result in a system that is no longer passive.

This paper aims to close the gap that exists between the theoretically ideal conditions in (1) on the one hand and the existing detailed analyses of basic two-channel controllers on the other hand [7]–[11]. Note that the Position-Force controller is considered here most representative for the transparency and stability problems of basic controllers.

Starting from these two ends of the spectrum, Fig. 1 gives an abstract illustration of two different approaches to obtain a real and well-performing teleoperation system. The first approach starts from the ideal conditions in (1) and would theoretically result in a perfectly transparent system. This system forms the starting point and is represented by the red cross at the complete right end of the transparency axis. However, due to practical problems, such as errors on the estimation of the dynamic models or the presence of filters to reduce the effect of signal noise, the stability of this system is not guaranteed in practice. Hence, in order to obtain a guaranteed stable system despite these practical problems, transparency has to be decreased. This can, for example, be done by adding extra damping at the master or by decreasing the value of a

All authors are with the Department of Mechanical Engineering, KU Leuven, Belgium e-mail: (see http://www.mech.kuleuven.be/en/pma/research/ras/About).

Manuscript received June 12, 2012; revised ??

scaling factor. These actions are represented by the red arrows pointing to the grey zone. This grey zone represents the best transparency that is practically feasible.

The second approach starts from a basic controller such as the Position-Force controller and seeks to extend this controller in order to improve both the transparency and stability properties. The relevant question is whether there are extensions that improve the transparency in the direction of this best, practically feasible, transparency, while also improving the stability. Such an extension would be represented by the green dashed arrow.

The choice for the first or the second approach also affects the complexity of the control analysis. Following the first approach, a number of previous control design efforts [3], [13], [14], started from the general control laws as defined by the extended four-channel framework:

$$F_m = -C_4 v_e - C_m v_h + C_6 F_h - C_2 F_e, \quad (2)$$

$$F_s = -C_s v_e + C_1 v_h + C_3 F_h - C_5 F_e, \quad (3)$$

$$\text{with } C_i = (K_{DD,i} s^2 +)\ K_{D,i} s\ +\ K_{P,i}\ (+\frac{K_{I,i}}{s}). \quad (4)$$

This means that the behaviour of the teleoperation system depends on a lot of parameters, which urges the use of numerical analyses. In contrast to this, the second approach minimizes the number of parameters for the system by starting from simple control laws, which facilitates analytic analyses and also the intuitive understanding of the obtained results.

Using the second approach, and starting from the known problems of the Position-Force controller, this paper presents a detailed transparency and stability analysis of the four-channel framework. This study reveals the importance of dynamic similarity of the master and slave device, as well as quantifies how practical issues like modelling errors and sensor noise introduce constraints on the admissible level of transparency.

Note that the analyses in this paper do not deal with the problem of time delay and don't explicitly assume position scaling. Also, when speaking about stability, it refers to coupled stability with a human operator and an environment in the continuous-time domain.

Section II describes the transparency and stability metrics used in this paper. Using these metrics, Section III summarizes the limitations of the Position-Force controller, while Section IV describes in detail two extensions of the Position-Force controller. The practical robustness of these extensions is addressed in Section V. The derived findings are discussed in Section VI. This paper ends with experimental results and conclusions in Section VII and VIII, respectively.

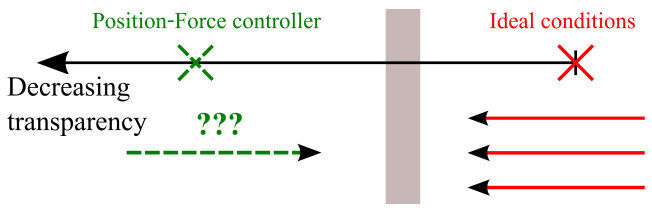

Fig. 1. To obtain a real and well-performing teleoperation system (the grey zone) one can either start from the ideal conditions (solid lines) or from a simple Position-Force controller and extend this (dashed lines).

TABLE I
PARAMETERS OF THE EXPERIMENTAL 1-D.O.F. TELEOPERATION SYSTEM

Model				Controller			
M_m:	0.64 kg	M_s:	0.61 kg	K_v:	80 Ns/m	μ:	1
B_m:	3.4 Ns/m	B_s:	11Ns/m	K_p:	4000 N/m	λ:	1

II. TRANSPARENCY AND STABILITY METRICS

The dynamic properties of a teleoperation system are often represented by a hybrid matrix **H** which defines the relation between the port variables (F_h,v_h) and (F_e,v_e) as follows:

$$\begin{bmatrix} F_h \\ -v_e \end{bmatrix} = \begin{bmatrix} h_{11} & h_{12} \\ h_{21} & h_{22} \end{bmatrix} \begin{bmatrix} v_h \\ F_e \end{bmatrix}.$$

These port variables (F_h,v_h) and (F_e,v_e) are the force and the velocity at the interaction interface with the human operator and with the environment, respectively.

Another approach is to look at the dynamic properties of the combination of the teleoperation system and the environment. The admittance describing the behaviour of this one-port system is referred to as Y_{MS} and can be written as a function of the parameters of the hybrid matrix and the impedance of the environment Z_e:

$$Y_{MS} = \frac{v_h}{F_h} = \frac{h_{22} Z_e + 1}{(h_{22} Z_e + 1) h_{11} - h_{12} h_{21} Z_e}. \quad (5)$$

This admittance directly describes the system with which the human operator interacts.

For a 1-d.o.f. system, the following equations of motion apply when assuming a rigid-body master and slave:

$$F_h + F_m = (M_m s + B_m^h) v_m, \quad (6)$$

$$F_s - F_e = (M_s s + B_s) v_s, \quad (7)$$

with F_m and F_s the actuator forces. Since the master and slave are modelled as rigid bodies, the velocities v_m and v_s (the velocities of the actuators) are equal to v_h and v_e respectively (the velocities of the end-effectors).

All illustrations in the remainder of this paper that form either numerical representations of analytic conditions or representations of numerical calculations, use the control and hardware parameters summarized in Table I. These parameters are based on the 1-d.o.f. experimental master-slave setup described in Section VII.

A. Transparency Metrics

To quantify transparency, multiple properties of Y_{MS} can be studied. In this paper, the two properties that are focused on are referred to as *free space transparency* and *stiffness transparency*:

$$Y_{MS(Z_e=0)}, \quad (8)$$

$$\lim_{s \to 0} \frac{1}{s} Y_{MS(Z_e = \frac{K_e}{s})}. \quad (9)$$

The former refers to what the human operator feels when the slave moves in free space, while the latter refers to the (quasi-static) relation between the stiffness the human operator feels and the actual stiffness of the environment.

The choice to focus on these two transparency metrics[1] is motivated by the fact that the intended application for the research presented in this paper is telesurgery.

B. Stability Metrics

A robust approach to study the stability of a teleoperation system is to use passivity theory. Based on this theory, the absolute stability method [7], [16] has been used extensively. Absolute stability is a sufficient condition for stable interaction with all passive environments and all passive operators as long as there is no direct interaction between the latter. In this paper, *Llewellyn's stability criteria* [16] are used to evaluate absolute stability.

The absolute stability method considers the teleoperation system itself and requires no information about the human operator or the environment. Despite this attractive property, the method has some drawbacks:

- The outcome is mostly binary. No qualitative or intuitive metric on the degree of absolute stability is provided.
- It is known to be conservative since it assumes an infinite dynamic range for both the environment and the operator.

Because of these drawbacks, several methods that allow to include bounds on the environment and/or human operator have been presented [9], [17], [18]. In this paper, the *bounded environment passivity* method is used [9], which studies the passivity of the admittance Y_{MS}. To do so, the positive real part condition is calculated with the model structure for the environment defined to be a pure stiffness. The motivation for focusing on the case of a pure stiffness is the fact that, for the envisioned controllers, stability problems are mostly noticed for hard contacts and a pure stiffness is a good and simple model for a hard contact.

III. Issues of the Position-Force controller

Using the above defined metrics, this section summarizes the fundamental transparency and stability limits of the Position-Force controller described in literature [9]–[11]. For this controller, the actuator forces can be defined as follows:

$$F_m = -\lambda F_e - B_m^c v_m \ , \tag{10}$$

$$F_s = (K_v s + K_p)(\mu x_m - x_s) \ , \tag{11}$$

with μ and λ the position and force scaling factors. B_m^c represents the master damping created by control, while B_m^h in (6) represented the physical damping of the master. In most cases, they can be combined in the parameter B_m.

This control definition will be referred to as the **PD-F** scheme and results in the following parameters for the extended four-channel framework:

$$C_s = (K_v + \frac{K_p}{s}),\ C_1 = \mu C_s,\ C_2 = \lambda,\ C_m = B_m^c$$
$$C_3 = C_4 = C_5 = C_6 = 0. \tag{12}$$

[1]These two transparency metrics describe the minimal impedance felt by the human operator as well as what the largest stiffness is the operator can feel, i.e. (9) for $K_e \rightarrow \infty$. In other words, they are very related to the concept of the Z-width, which describes the dynamic range of achievable impedances [15].

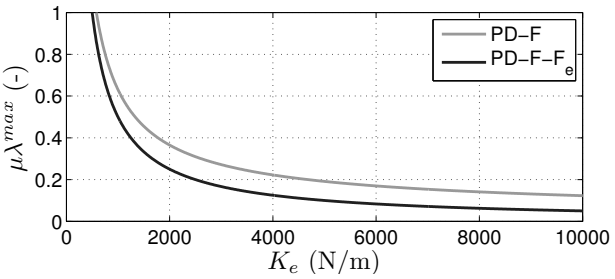

Fig. 2. Bounded environment passivity: The maximum value for $\mu\lambda$ as a function of the range of environment stiffnesses for the **PD-F** and the **PD-F-F**$_e$ scheme.

For this controller, the two transparency metrics are:

$$Y_{MS(Z_e=0)} = \frac{1}{M_m s + B_m}, \tag{13}$$

$$\lim_{s\rightarrow 0} \frac{1}{s} Y_{MS(Z_e=\frac{K_e}{s})} = \frac{K_p + K_e}{\mu\lambda(K_p K_e)}. \tag{14}$$

Hence, in free space, the user feels the full dynamics of the master but not those of the slave. The limitation is the stiffness transparency. Even in case $\mu\lambda = 1$, the user does not feel the actual environment stiffness but the series connection of the control stiffness K_p and the environment stiffness.

In [9], it was proven that this controller results in a teleoperation system that is never two-port passive nor absolutely stable. Also in [9], using the bounded environment passivity method, relation (15) between the scaling factor and the environment stiffness was derived. For the parameters of Table I, this relation is shown in Fig. 2. Clearly, only for (very) soft environments, a value of $\mu\lambda$ close to 1 is allowed. For larger stiffnesses, this value has to be significantly smaller, which further reduces the stiffness transparency.

The analyses in [9]–[11] demonstrated that the fundamental stability limits of the Position-Force controller originate from any kind of lag between the master and slave.

The main limitations of the **PD-F** scheme:

- The human operator feels the series connection of the control stiffness and the environment stiffness.
- For stability reasons and depending on the system parameters, a value of $\mu\lambda$ close to 1 is not allowed if a wide range of environments is envisioned.

IV. Improving transparency and/or stability

This section describes extensions of the Position-Force controller and studies the transparency and stability properties of these extensions. All extensions fit in the extended four-channel framework, but as far as the authors are aware of, no detailed analyses have been presented for these controllers. Hence, the here presented comprehensive description of their properties in combination with an intuitive explanation extends the state-of-the-art.

A. Local force feedback

As above, perfect stiffness transparency cannot be obtained with the **PD-F** scheme due to the practical limit on the

$$\textbf{PD-F:} \qquad \mu\lambda \leq \frac{B_m(B_s+K_v)}{K_e^{max}M_sK_v^2}\Big((B_s+K_v)K_v - 2M_sK_p + 2\sqrt{M_s(M_sK_p^2 - K_pK_vB_s + K_v^2K_e^{max})}\Big). \quad (15)$$

$$\textbf{PD-F-F}_e\textbf{:} \qquad \mu\lambda \leq \frac{B_m(B_s+K_v)}{K_e^{max}M_sK_v^2}\Big((B_s+K_v)K_v - 2M_sK_p + 2\sqrt{M_s(M_sK_p^2 - K_pK_vB_s)}\Big) \quad (16)$$

$$\textbf{PD-F-F}_e\ (\gamma)\textbf{:} \qquad \mu\lambda \leq -\frac{B_m(B_s+K_v)(B_s(1-\gamma)+(2M_sK_p-K_v)(\mu-1)+B_sK_v(2-\gamma-\mu)-2\sqrt{\text{root}})}{K_e^{max}M_s(B_s(1-\gamma)+K_v(1-\mu))^2} \quad (17)$$

$$\text{root} = B_s^2(\gamma^2-\gamma-\gamma\mu+\mu) + K_vB_s(\gamma\mu-\gamma+\mu-\mu^2) + M_sK_p(1-\mu)^2 \quad (18)$$

controller stiffness K_p[2]. In order to improve the stiffness transparency without increasing K_p, local force feedback at the slave can be considered:

$$F_s = (K_vs+K_p).(\mu x_m - x_s) + F_e \quad (19)$$

$$\text{i.e.} \quad (12) \quad \text{and} \quad C_5 = -1 \quad (20)$$

This controller will be referred to as the **PD-F-F**$_e$ scheme. The free space transparency is the same as for the **PD-F** scheme, while the stiffness transparency is optimal now in case $\mu\lambda$ would be set to 1:

$$Y_{MS(Z_e=0)} = \frac{1}{M_ms+B_m}, \quad (21)$$

$$\lim_{s\to 0}\frac{1}{s}Y_{MS(Z_e=\frac{K_e}{s})} = \frac{1}{\mu\lambda(K_e)}. \quad (22)$$

However, the coupled stability problems become worse. Using the bounded environment passivity method, the relation between the scaling factor and the environment stiffness is derived and given in (16). This relation is shown in Fig. 2 for the parameters of Table I. This figure shows that the maximum values for $\mu\lambda$ for large environment stiffnesses are even smaller compared to those for the **PD-F** scheme.

Note that in [4], Hashtrudi-Zaad and Salcudean claimed that this local force feedback improves *stability*, but they are not referring to the *coupled stability* property. Their claim is motivated by (1) the idea that local force feedback improves the local contact stability and by (2) considering that a local force feedback channel replaces an actual communication channel which should improve the robustness with respect to time-delay.

Conclusion on the **PD-F-F**$_e$ scheme:

- The operator no longer feels the series connection of the control stiffness and the actual environment stiffness, but, the restriction on the achievable value of $\mu\lambda$ is even worse.

B. Local model-based feedforward

As mentioned before, the stability problems of the Position-Force controller originate a.o. from the limited bandwidth of the position-controlled slave. A way to circumvent bandwidth limitations is to use model-based feedforward. The following control law combines local force feedback with model-based feedforward:

$$F_s = (K_vs+K_p).(\mu.x_m - x_s) + F_e + (\tilde{M}_s s^2 + \tilde{B}_s s)\mu x_m \quad (23)$$

$$\text{i.e. (12) and } C_5 = -1 \quad \text{and } C_1 = \mu(\tilde{M}_s s + \tilde{B}_s + C_s) \quad (24)$$

One can prove that this controller results in a *non-strictly* two-port passive, hence also absolutely stable, teleoperation system in the ideal situation that the parameters of the slave are correctly estimated ($\tilde{M}_s = M_s$ and $\tilde{B}_s = B_s$). This can be intuitively understood since under this assumption, the bandwidth of the position-controlled slave is theoretically infinitely high. Hence, when no time delay, no signal filters and ideal actuators and data acquisition systems are considered, there is no longer lag between the master and slave.

It is interesting to note that in case the dynamic model of the slave is exactly known and $\mu = \lambda = 1$, the control laws (23) and (10) result in a system for which three of the four ideal conditions (1) hold. Only the master dynamics are not cancelled. Hence, the admittance Y_{MS} becomes:

$$Y_{MS}(s) = \frac{1}{M_ms + B_m + Z_e} \quad (25)$$

However, because of inevitable modelling errors, the robustness of this approach is limited. To get a quantitative understanding of the robustness to modelling errors, the following scenario has been studied: assume that the slave damping B_s is exactly known and the estimated slave mass $\tilde{M}_s$ is a factor γ of the real slave mass M_s:

$$\tilde{M}_s = \gamma M_s \quad \text{and} \quad \tilde{B}_s = B_s. \quad (26)$$

An analytic analysis of the bounded environment passivity properties for the **PD-F-F**$_e$ scheme with model-based feedforward, results in a set of extensive conditions of which the most restrictive one is given in (17).

Fig. 3(a) shows this conditions as an upper boundary for the $\mu\lambda$ value as a function of the range of environment stiffnesses for five different values of γ. Fig. 3(b) shows the same condition but as an upper boundary for K_e as a function of γ in case $\mu = \lambda = 1$. Both figures are obtained for the parameters of Table I. These figures demonstrate how the factor γ has to approach 1 in order to obtain a significant improvement of the range of stiffnesses for which the controller results in a passive admittance Y_{MS}.

[2]The practical limit on K_p stems from the requirement for stability of the slave's local position controller.

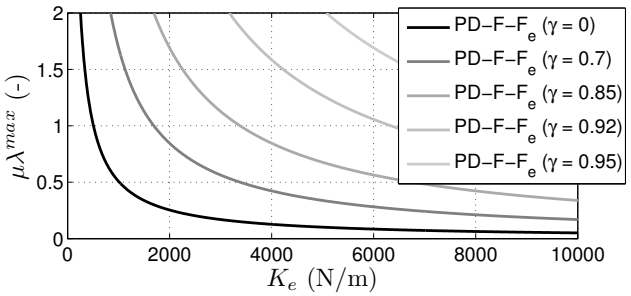

(a) The maximum value for $\mu\lambda$ as a function of the range of environment stiffnesses for different values of γ.

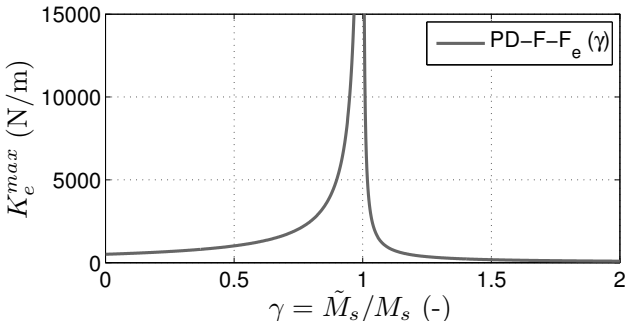

(b) The maximum value for K_e as a function of γ, i.e. the correctness of the estimated slave inertia.

Fig. 3. Bounded environment passivity for the **PD-F-F**$_e$ scheme with model-feedforward.

Conclusion on the use of model-based feedforward:

- Adding model-based feedforward to the **PD-F-F**$_e$ scheme only significantly improves the stability, in case the dynamic model of the slave is accurately known.

C. A third channel

So far, two-channel controllers have been discussed. The local force feedback extension addressed the transparency issue, while the model-based feedforward extension addressed the stability issue. Another way to address both issues is to use a third-channel as in the following control law for the slave:

$$F_s = (K_v s + K_p).(\mu x_m - x_s) + F_h \quad (27)$$

$$\text{i.e.} \quad (12) \text{ and } C_3 = 1 \quad (28)$$

This controller will be referred to as the **PD-F-F**$_h$ scheme [19]. To understand the interesting properties of this three-channel controller, it is necessary to rewrite the equation of motion for the master, i.e. (6), as follows:

$$F_h = (M_m s + B_m^h) v_m - F_m. \quad (29)$$

After replacing F_m with the control input (10), this becomes:

$$F_h = (M_m s + B_m) v_m + \lambda F_e, \quad (30)$$

From this equation, it is clear that control law (27) indirectly comprises a model-based feedforward term, i.e. to improve the stability and a local force feedback term, i.e. to improve the transparency. As such, if $\mu = 1$ and if the master and slave are dynamically similar, this control law can significantly improve both the stability and transparency. Note that in the remainder of this section all claims implicitly assume $\mu = 1$.

In contrast to the approach of using model-based feedforward, the master has to be equipped with a force sensor at the end-effector, but no accurate estimation of the master and slave dynamics is required.

With this control definition, the free space transparency is the same as for the **PD-F** and **PD-F-F**$_e$ scheme, while the stiffness transparency is defined as follows:

$$\lim_{s\to 0} \frac{1}{s} Y_{MS(Z_e=\frac{K_e}{s})} = \frac{K_p + (1-\lambda)K_e}{\mu\lambda(K_p K_e)}. \quad (31)$$

Therefore, the stiffness transparency is optimal if λ can be 1.

One can prove that this controller results in a non-strictly two-port passive teleoperation system for the specific situation that the dynamic parameters of the master and slave are exactly the same ($M_m = M_s$ and $B_m = B_s$) in case $\mu = \lambda = 1$. To further analyse this controller, an absolute stability study was performed. Appendix A describes the resulting conditions.

The finding that the **PD-F-F**$_h$ scheme results in a non-strictly two-port passive teleoperation system in case $M_m = M_s$, $B_m = B_s$ and $\mu = \lambda = 1$, indicates that having similar dynamic properties for the master and slave has a positive impact on the absolute stability properties. Recall that this was already suggested by the interpretation of (30).

An obvious question then is how to quantify this need for dynamic similarity of the master and slave. To look into this, Fig. 4 shows for which values of $\frac{M_s}{M_m}$ and $\frac{B_s}{B_m}$, the teleoperation system is absolutely stable based on the conditions given in Appendix A. Again the parameters for the controller and the master dynamics are taken from Table I.

This figure illustrates that there is no straightforward condition that answers this question, but at least there is a clear trend noticeable, namely that the bounds on the ratio of the inertias are much more restrictive than the bounds on the ratio of the damping values. Extra calculations for other values of the controller (K_p = 100 $\rightarrow$ 10000 N/m) or the master dynamics (M_m = 0.2 $\rightarrow$ 4 kg), all show the same trend. Hence, a similar value for the inertia of the master and slave is an important requirement for the three-channel controller studied here.

Note finally that Fig. 4 illustrates how the requirements for the master and slave dynamics get more restrictive, the closer the value of λ gets to one. For the special case that $\mu = \lambda = 1$, the region of absolute stability has shrunk to a point. This in itself is yet another illustration of the well-known trade-off between stability and transparency: the more demanding the transparency requirements, the more demanding the stability conditions are.

Conclusion on the use of the third channel:

- It directly improves the stiffness transparency in a similar way as local force feedback did.
- It improves the stability in case the dynamic properties, especially the inertias, of the master and slave are similar.

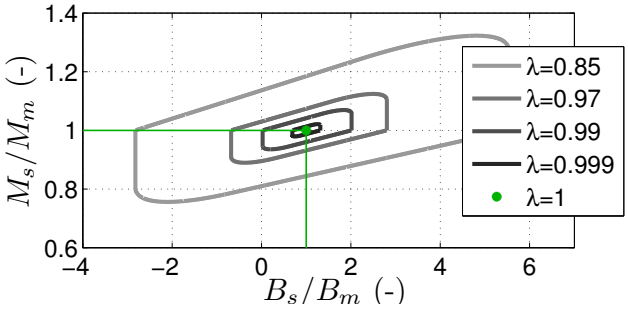

Fig. 4. Absolute stability for the **PD-F-F**$_h$ scheme: the conditions (39) to (38) defining the regions of parameters that result in an absolutely stable teleoperation system.

V. Robustness to filtering

In the previous section, the **PD-F-F**$_e$ scheme in combination with model feedforward and the **PD-F-F**$_h$ scheme have been described. This section quantifies to what extent these controllers are robust with respect to signal filters.

Using model-based feedforward requires the knowledge on the acceleration of the master. In case this acceleration is obtained by taking the second derivative of a quantized position measurement, significant filtering of the acceleration signal is typically required. Therefore, for the **PD-F-F**$_e$ scheme with model-based feedforward, the effect of a 1st-order low-pass filter on the acceleration term is calculated. To do so, the last term of equation (23) is replaced by the following:

$$... + (\tilde{M}_s s^2 \frac{x_m}{s/\omega_c + 1} + \tilde{B}_s s\ x_m), \tag{32}$$

with ω_c being the cut-off frequency of the filter (expressed in rad/s).

Similarly, force sensors suffer from signal noise, which might require filtering as well. Therefore, for the **PD-F-F**$_h$ scheme, the effect of low-pass filtering the force signals is analyzed. Hereto, F_e and F_h are replaced in (10) and (27) as follows:

$$F_e \quad \rightarrow \quad \frac{F_e}{s/\omega_c + 1}\ , \qquad F_h \quad \rightarrow \quad \frac{F_h}{s/\omega_c + 1} \tag{33}$$

For both extensions, the positive real part conditions of the resulting admittance $Y_{MS(K_e)}$ takes the form of a 4th order polynomial inequality in ω^2. Consequently, an analytic analysis becomes too complex and the analysis is performed numerically as follows: starting from $K_e = 0$, the condition $\Re(Y_{MS(K_e)}(j\omega)) \geq 0$ is verified for $\omega \in [0.1 - 10^9 rad/s]$ for increasing values of K_e (increment: 1 N/m). When the condition $\Re(Y_{MS(K_e)}(j\omega)) \geq 0$ no longer holds, K_e^{max} is obtained. This is done here for different values of the bandwidth of the low-pass filter (bandwidth = $\frac{\omega_c}{2\pi}$) and the parameters of Table I, i.e. with $\mu = \lambda = 1$.

Fig. 5(a) shows the results of these calculations for the **PD-F-F**$_e$ scheme with model-based feedforward and for two different values of the factor γ. In case $\gamma = 1$, it was stated before that the resulting teleoperation system is two-port passive. This can be seen here by the fact that for very large bandwidths, the maximum environment stiffness does not seem to be limited. In case $\gamma = 0.8$, there is a limit for K_e^{max}

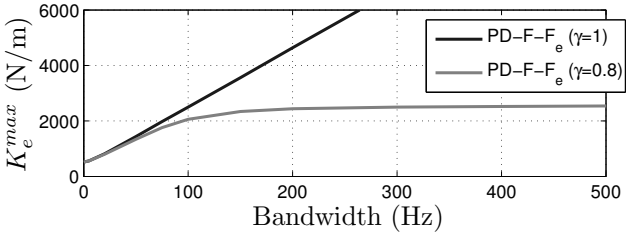

(a) The **PD-F-F**$_e$ scheme: effect of filtering acceleration

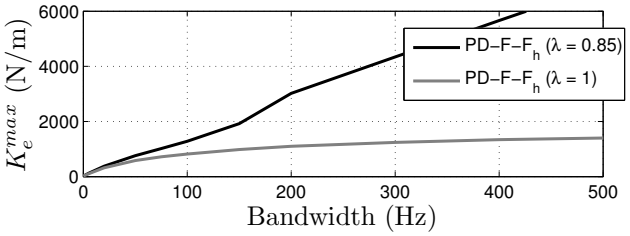

(b) The **PD-F-F**$_h$ scheme: effect of filtering force

Fig. 5. Bounded environment passivity: the maximum environment stiffness for which the admittance $Y_{MS(K_e)}$ is passive as a function of the bandwidth of the low-pass filter.

at 2540 N/m, independent of the filter's bandwidth. Note that this value can be calculated using (17).

Fig. 5(b) shows these results for the **PD-F-F**$_h$ scheme for two values of λ. If $\lambda = 1$, the resulting teleoperation system is not absolutely stable as can be verified using the conditions in Appendix A. In that case there is a limit for K_e^{max} at 1560 N/m, independent of the filter's bandwidth. With $\lambda = 0.85$, one can see from Fig. 4, that the resulting teleoperation system is absolutely stable. Again, this can be seen here by the fact that for very large bandwidths, K_e^{max} does not seem to be limited.

From both figures, it is clear that the low-pass filter has a negative effect on K_e^{max}. The negative effect of the filter on the acceleration signal for the **PD-F-F**$_e$ scheme is, furthermore, similar to the effect of filters on the force signals for the **PD-F-F**$_h$ scheme.

VI. Discussion

As mentioned in Section III, the restricted bandwidth of the position-controlled slave is an important source of lag between the master and the slave. This source has not always been explicitly addressed in literature, since a lot of works focus on the problem of time-delay. For a lot of applications, however, time delay is not the (only) issue.

The two extensions discussed in detail in this paper address the problem of this restricted bandwidth by means of feedforward. The first extension with the model-based feedforward does this explicitly by making use of the dynamic model of the slave, while the **PD-F-F**$_h$ scheme does this implicitly by making use of a third channel. Which one of these extensions is preferable is application-specific and depends on the following aspects:

- Can a good dynamic model be obtained?
- Is the use of force sensors an option? What will be the signal quality?

- Can the master and slave be dynamically similar?

The possible need for a dynamically similar master and slave illustrates how the required hardware properties can depend on the controller of choice and vice versa. The quality of the sensors relates to the requirement for (a specific bandwidth of) a filter. As mentioned also in [9], the above concerns motivate the need for a mechatronic approach to the design of teleoperation systems, i.e. a concurrent design of the hardware and controller. Based on this conclusion, the authors developed a 3-d.o.f. teleoperation system that has keyhole surgery as the intended application [20]. Testing of this system indicated that 1-d.o.f. approximations can provide reliable design/tuning guidelines also for a non-linear multi-d.o.f. system.

The finding on the effect of filters is representative for a general issue of designing controllers for teleoperation systems: when only considering basic representations for the hardware and the controller of a teleoperation system, there are controller and/or hardware combinations that theoretically result in excellent stability and transparency properties. However, practical issues can significantly worsen these properties. Next to the presence of filters, other practical issues are the presence of structural compliance, a limited bandwidth of the motor drives or a limited sample time. The common denominator of these issues, is the fact that they increase the lag in a part of the teleoperation loop.

VII. Experimental results

The experiments described in this section are performed on a 1-d.o.f. master-slave setup. The goal of the experiments is to illustrate the superior stiffness transparency of the **PD-F-F**$_h$ scheme compared to the traditional Position-Force controller, i.e. the **PD-F** scheme. The **PD-F-F**$_h$ scheme is chosen here, since the master and slave have a similar mass and the quality of the position sensor of the master is poor, which means the signal-to-noise of the acceleration signal is really poor. First, the experimental setup is described in more detail.

A. The experimental setup

The 1-d.o.f. master-slave setup, described in more detail in [9], consists of two current-driven voice coil motors. On both devices, one-dimensional force sensors are mounted at the end-effector. Table I gives an overview of the parameters used for the rigid-body models and the controllers. The controllers are implemented on a dSpace board running a real-time control loop with a frequency of 1 kHz.

B. The results

The experiment shows the interaction of a human operator with a hard environment ($\pm$41000 N/m) and a soft environment (1100 N/m) for two controllers.

The first controller is the **PD-F** scheme with the parameters of Table I. As can be derived from (15), the admittance $Y_{MS(K_e)}$ is active for both the soft and the hard environment. Especially for the hard environment, the interaction is mostly unstable. It is, however, not impossible for a human operator to realize a stable interaction even with the hard environment, albeit this requires *effort*.

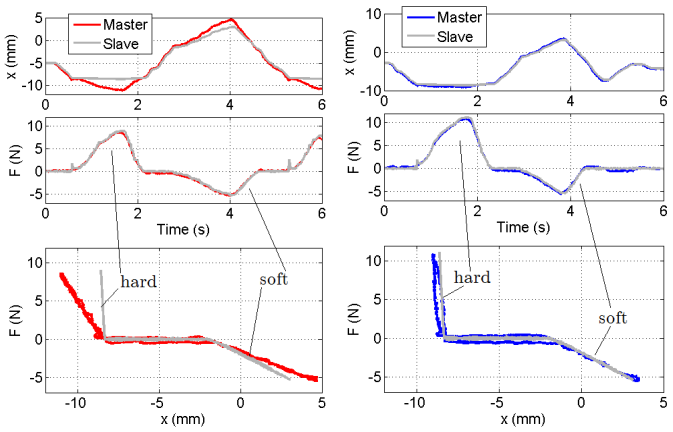

(a) The **PD-F** scheme (b) The **PD-F-F**$_h$ scheme

Fig. 6. Interaction with a hard contact ($\pm$41000 N/m) and a soft object (1100 N/m) for (a) the **PD-F** scheme and (b) the **PD-F-F**$_h$ scheme.

The second controller is the **PD-F-F**$_h$ scheme with the parameters of Table I and $B_m = 13$ instead of 3.4 Ns/m. This means virtual damping (B_m^c) has been added. In IV-C, it was shown that if $\mu = \lambda = 1$, both the inertia and the damping of the master and the slave should be similar in order to obtain a stable system. Compared to the first controller, the second controller thus guarantees stable interaction with all environment stiffnesses and also provides perfect stiffness transparency. The free-space feeling, however, is worse due to the large master damping B_m, that is required because of the inherently large slave damping.

For both controllers an interaction experiment is shown in a position-time, a force-time and a force-position plot. Fig. 6(a) and 6(b) show these plots for the first and the second controller, respectively. All interactions seem stable, but as mentioned before, this required some *effort* of the human operator for the first controller and the hard environment.

One can see that the stiffness felt with the first controller is clearly lower than the real environment stiffness due to the limited control stiffness K_p. As defined by (14), the operator feels the series connection of the real environment stiffness and the control stiffness. With the second controller, on the other hand, the environment stiffness is more accurately reflected to the human operator. Hence, these experiments illustrate the interesting properties of the **PD-F-F**$_h$ scheme, i.e. achieving perfect stiffness transparency while guaranteeing stable interaction for a large range of environment stiffnesses.

VIII. Conclusion

This paper bridges the gap between existing detailed analysis of basic two-channel controllers and the ideal conditions of the four-channel framework.

It is quantitatively demonstrated how hard it is to obtain close to perfect transparency, even in the absence of time delay. For the two analyzed extensions of the Position-Force controller, either an accurate dynamic model is required or the master and slave have to be dynamically similar. Furthermore, it is shown how the simple presence of a low-pass filter can deteriorate the interesting properties.

$$M_s \leq -\frac{\left(\lambda B_m-\lambda\mu K_v-2B_m-2\sqrt{-\lambda^2 B_m\mu K_v+(1-\lambda)B_m^2+\lambda B_m\mu K_v}\right)M_m(B_s+K_v)}{\lambda(B_m+\mu K_v)^2}, \tag{34}$$

$$M_s \geq -\frac{\left(\lambda B_m-\lambda\mu K_v-2B_m+2\sqrt{-\lambda^2 B_m\mu K_v+(1-\lambda)B_m^2+\lambda B_m\mu K_v}\right)M_m(B_s+K_v)}{\lambda(B_m+\mu K_v)^2}, \tag{35}$$

$$M_s \leq \frac{-1}{2\mu^2\lambda K_p}\Big(-\lambda\mu^2 B_s K_v+(((3K_v+B_s)B_m-2M_m K_p)\lambda-(2(B_s+K_v))B_m)\mu+\lambda B_m^2 \tag{36}$$
$$\cdots-\sqrt{\lambda((\mu K_v+B_m)^2-4\mu M_m K_p)).(\lambda\mu^2 B_s^2+(2((B_s+2K_v)\lambda-2(B_s+K_v)))B_m\mu+\lambda B_m^2)}\Big),$$

$$M_s \geq \frac{+1}{2\mu^2\lambda K_p}\Big(-\lambda\mu^2 B_s K_v+(((3K_v+B_s)B_m-2M_m K_p)\lambda-(2(B_s+K_v))B_m)\mu+\lambda B_m^2 \tag{37}$$
$$\cdots+\sqrt{\lambda((\mu K_v+B_m)^2-4\mu M_m K_p)).(\lambda\mu^2 B_s^2+(2((B_s+2K_v)\lambda-2(B_s+K_v)))B_m\mu+\lambda B_m^2)}\Big),$$

$$M_s^{bound} = \frac{\left(2B_m K_v^2(\lambda-1)(\mu\lambda K_v+B_m)-\lambda K_p M_m(K_v(\lambda\mu B_s+(\lambda-2)B_m)+\mu\lambda B_s^2)+B_s B_m\left(2(\lambda-1)(2B_m K_v+2\mu\lambda K_v^2+\mu\lambda B_s K_v+B_s B_m)+\lambda(2-\lambda)K_p M_m\right)\right)}{\lambda K_p(3\lambda B_m\mu K_v-\lambda\mu^2 B_s K_v-2B_m\mu K_v+\lambda B_m^2+\mu(\lambda-2)B_s B_m)} \tag{38}$$

The experimental results presented in this paper, demonstrate the restricted stiffness transparency of the Position-Force controller, as well as how the extensions provide nearly perfect stiffness transparency.

Finally, this paper should help the intuitive understanding of the (theoretical) possibilities of the four-channel framework and the awareness for its practical feasibility.

APPENDIX A

For the **PD-F-F**$_h$ scheme, the most critical of Llewellyn's criteria can be written as a second order polynomial inequality in ω^2 of the form $ax^2+bx+c \geq 0, \forall x=\omega^2 \geq 0$. This condition simplifies to $a \geq 0$, $c \geq 0$ and ($b^2-4ac \leq 0$ or $b \geq 0$). Most of the resulting conditions can be expressed as boundaries for the slave inertia M_s. $a \geq 0$ results in the conditions (34) and (35), while $b^2-4ac \leq 0$ results in the conditions (36) and (37), and $b \geq 0$ results in these conditions:

$$B_s < B_s^{asympt} \quad : \quad M_s \geq M_s^{bound}, \tag{39}$$

$$B_s > B_s^{asympt} \quad : \quad M_s \leq M_s^{bound}, \tag{40}$$

$$\text{with} \quad B_s^{asympt} = \frac{-B_m(3\mu\lambda K_v+\lambda B_m-2\mu K_v)}{(\mu(\lambda B_m-\mu\lambda K_v-2B_m)}, \tag{41}$$

and M_s^{bound} given by condition (38). The condition $c \geq 0$, finally, can be expressed as a lower boundary for K_v:

$$K_v \geq -\frac{\lambda(B_m+\mu B_s)^2-4\mu B_s B_m}{4\mu B_m(-1+\lambda)}. \tag{42}$$

ACKNOWLEDGMENT

This work was supported by a PhD grant from the Institute for the Promotion of Innovation through Science and Technology in Flanders (I.W.T.-Vlaanderen). The authors would like to thank also Prof. J. De Schutter and Prof. G. Niemeyer for their valuable comments on the manuscript.

REFERENCES

[1] G. R. Raju, G. Verghese, and T. Sheridan, "Design issues in 2-port network models of bilateral remote manipulation," in *Proceedings of the IEEE International Conference on Robotics and Automation*, vol. 3, Scottsdale, AZ, May 1988, pp. 1316–1321.

[2] D. Lawrence, "Stability and transparency in bilateral teleoperation," *IEEE transactions on robotics and automation*, vol. 9, no. 5, pp. 624–637, October 1993.

[3] Y. Yokokohji and T. Yoshikawa, "Bilateral control of master-slave manipulators for ideal kinesthetic coupling," *IEEE transactions on robotics and automation*, vol. 10, no. 5, pp. 605–620, October 1994.

[4] K. Hashtrudi-Zaad and S. Salcudean, "On the use of local force feedback for transparent teleoperation," in *Proc. of The IEEE Int. Conf. on Robotics and Automation*, Detroit, Michigan, May 1999, pp. 1863–1869.

[5] I. Aliaga, A. Rubio, and E. Sanchez, "Experimental quantitative comparison of different control architectures for master-slave teleoperation," *IEEE Transactions on Control Systems Technology*, vol. 12, no. 1, pp. 2–11, January 2004.

[6] E. Naerum and B. Hannaford, "Global transparency analysis of the lawrence teleoperator architecture," in *Proc. of The IEEE Int. Conf. on Robotics and Automation*, Kobe, Japan, May 2009, pp. 4344–4349.

[7] K. Hashtrudi-Zaad and S. Salcudean, "Analysis of control architectures for teleoperation systems with impedance/admittance master and slave manipulators," *The international Journal of Robotics Research*, vol. 20, no. 6, pp. 419–445, June 2001.

[8] M. Tavakoli, A. Aziminejad, R. Patel, and M. Moallem, "Enhanced transparency in haptics-based master-slave systems," in *Proc. of the American Control Conf.*, NY, USA, July 2007, pp. 1455–1460.

[9] B. Willaert, B. Corteville, D. Reynaerts, H. Van Brussel, and E. Vander Poorten, "A mechatronic analysis of the classical position-force controller based on bounded environment passivity," *The Int. J. of Robotics Research*, vol. 30, no. 4, pp. 444–462, April 2011.

[10] R. Daniel and P. McAree, "Fundamental limits of performance for force reflecting teleoperation," *The International Journal of Robotics Research*, vol. 17, no. 8, pp. 811–830, August 1998.

[11] P. Shull and G. Niemeyer, "Force and position scaling limits for stability in force reflecting teleoperation," in *Proc. of the ASME Dynamic Systems and Control Conf.*, Ann Arbor, Michigan, USA, 2008, pp. 607–614.

[12] A. Haddadi and K. Hashtrudi-Zaad, "A new robust stability analysis and design tool for bilateral teleoperation control systems," in *Proceedings of the IEEE International Conference on Robotics and Automation*, Pasadena, CA, USA, May 2008, pp. 663–670.

[13] E. Vander Poorten, "Improving haptic fidelity for intuitive manipulation in scaled teleoperation and virtual environment," Ph.D. dissertation, University of Kyoto, 2007.

[14] H. Cho and J. Park, "Impedance control with variable damping for bilateral teleoperation under time delay," *JSME International Journal Series C*, vol. 48, no. 4, pp. 695–703, 2005.

[15] J. Colgate and J. M. Brown, "Factors affecting the z-width of a haptic display," in *Proceedings of the International Conference on Robotics & Automation,*, 1994, pp. 3205–3210.

[16] F. Llewellyn, "Some fundamental properties of transmission systems," in *Proc. IRE*, vol. 40, 1952, pp. 271–283.

[17] A. Peer and M. Buss, "Robust stability analysis of a bilateral teleoperation system using the parameter space approach," in *Proceedings of IEEE International Conference on Intelligent Robots and Systems*, Nice, France, September 2008, pp. 2350–2356.

[18] A. Haddadi and K. Hashtrudi-Zaad, "Bounded-impedance absolute stability of bilateral teleoperation control systems," *IEEE Transactions on Haptics*, vol. 3, no. 2, pp. 15–27, 2010.

[19] B. Willaert, B. Corteville, D. Reynaerts, H. Van Brussel, and E. Vander Poorten, "Transparency trade-offs for a 3-channel controller revealed by the bounded environment passivity method." in *Int. Conf. on Adv. in Computer-Human Interact. (ACHI)*, St. Maarten, Febr. 2010, pp. 66–72.

[20] B. Willaert, B. Corteville, D. Reynaerts, and H. Van Brussel, "A mechatronic approach towards bilateral teleoperation for keyhole surgery," in *Proceedings of ACTUATOR 2012*, Bremen, Germany, June 2012.